Molecular Catalysis 433 (2017) 20–27

Contents lists available at ScienceDirect

Molecular Catalysis

journal homepage: www.elsevier.com/locate/mcat

MCAT

Comparative investigation of the MTH induction reaction over HZSM-5 and HSAPO-34 catalysts

You Zhou[a,b], Liang Qi[a,b], Yingxu Wei[a], Zhongmin Liu[a,*]

[a] National Engineering Laboratory for Methanol to Olefins, Dalian National Laboratory for Clean Energy, iChEM (Collaborative Innovation Center of Chemistry for Energy Materials), Dalian Institute of Chemical Physics, Chinese Academy of Sciences, Dalian 116023, PR China
[b] University of Chinese Academy of Sciences, Beijing 100049, PR China

ARTICLE INFO

Article history:
Received 5 December 2016
Received in revised form 9 February 2017
Accepted 12 February 2017

Keywords:
HZSM-5
HSAPO-34
Methanol to hydrocarbons
Induction
Mechanism

ABSTRACT

Methanol to hydrocarbons (MTH) induction reaction was comparatively investigated over HZSM-5 and HSAPO-34 catalysts combined with on line thermogravimetry analysis of catalyst weight increment by intelligent gravimetric analyzer (IGA) studies. The influence of catalyst topology and acidity and reaction temperature on the reaction performance were correlated with the confined organics formation and evolution over the catalysts. For the latter stage of the MTH induction period, methanol conversion over HZSM-5 catalyst was proved a well-defined autocatalysis process, while over HSAPO-34, the increasing rate of methanol conversion was retarded due to accumulation of methyladamantanes. There existed a similar deactivation behaviour for HZSM-5 catalysts with low Si/Al ratios and HSAPO-34 catalysts during the temperature-programmed MTH (TP-MTH) reaction. But the IGA studies showed that the change of the retained species amount was quite different: for TP-MTH reaction over HZSM-5, the amount firstly increased and then decreased to a stable value; while for HSAPO-34, the amount kept increasing until reached a constant value. MTH induction reaction over HZSM-5 catalyst with different Si/Al ratios and HSAPO-34 catalysts with different Si contents were also investigated. All these findings revealed the influence of catalyst topologies on the formation of retained species and then on the catalyst activity during the MTH induction reaction.

1. Introduction

Light olefins and aromatics are very important basic chemical products in the world which are traditionally generated from the oil-based route. It's well-known to everyone that the oil reserves is being consumed in an accelerating rate, threatening the world energy safety consequently. In recent years, the methanol to hydrocarbons (MTH) process over HSAPO-34 and HZSM-5 catalysts has received great success in commercialization and that has been proved to be a perfect alternative to guarantee the generation of the basic chemicals, since methanol could be simply mass-produced from natural gas, coal, and biomass [1–4].

The MTH reaction is a very complicated and interesting process during which the methanol molecular without C-C bond can be efficiently transformed into kinds of hydrocarbon products including alkanes, olefins and aromatics, etc. Considering the interesting transformation process, a lot of research has been done to make clear the formation of the first C-C bond [5–17], but it seems difficult to reach a popularly convincing conclusion due to the shortage of very powerful experimental evidence and the debate may still proceed on. Moreover, considering the rather complicated reaction network, it is almost impossible to make clear every elemental step. Concerning the change of apparent catalyst activity, the whole reaction process can be divided into induction period, high methanol conversion period and the deactivation period [4,18]. A deep and clear recognition of the reaction mechanism is necessary for a comprehensive understanding of the changing catalyst activity.

Since the discovery of the MTH reaction in 1970s, about 20 distinct methanol conversion mechanisms have been proposed [1,3,4,8,19–26]. Up to now, the "hydrocarbon pool" (HCP) mechanism has received popular support from both experimental and theoretical investigation and can offer a reasonable explaination for the existence of the induction period [22,27,28]. According to the HCP mechanism, a certain amount of organic species should be generated and retained in the catalyst channels or cages acting as the reaction centers, to which methanol is added and olefins are eliminated in a closed catalytic cycle [1–4]. However, besides the active HCP species, some inactive and poorly mobile polycyclic species

* Corresponding author.
E-mail address: liuzm@dicp.ac.cn (Z. Liu).

http://dx.doi.org/10.1016/j.mcat.2017.02.018
2468-8231/

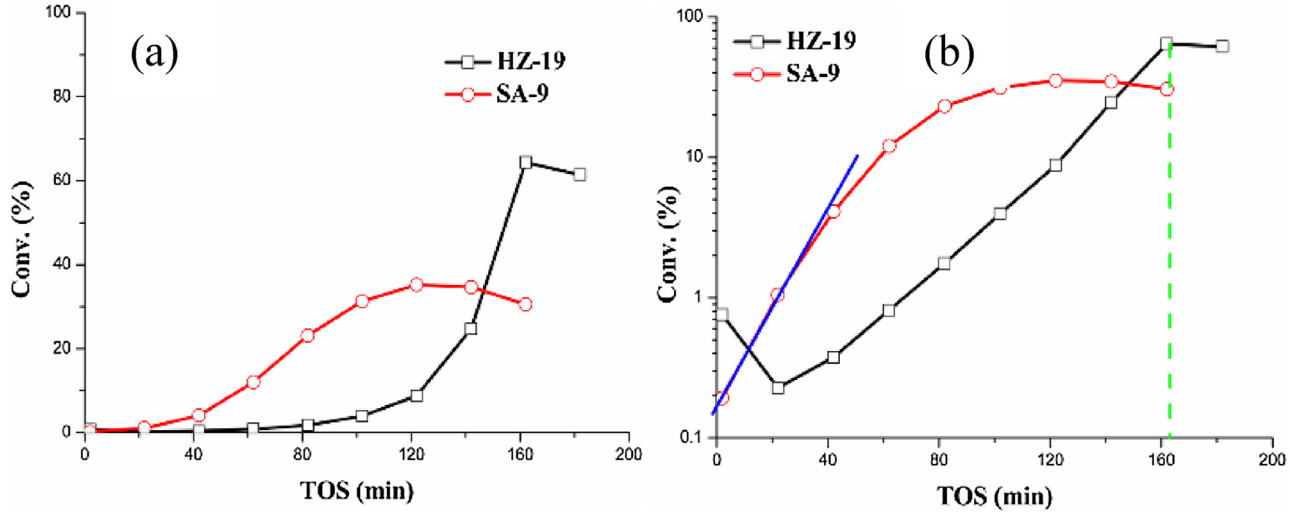

Fig. 1. Conversion of methanol on HZ-19 and SA-9 at 260 °C as a function of TOS. The y axis is in a logarithmic scale for (b).

would also be unavoidably generated during the high methanol conversion period and consequently leaded to the catalyst deactivation. Besides the proposal of the basic HCP mechanism, more detailed mechanism has been proposed and added to make the HCP mechanism work more effective. The side-chain alkylation and the paring mechanism provided two possible routes of how olefin products are generated from methylbenzenes which act as the active species [20,29]. Moreover, Olsbye et al. later found that both methylbenzenes and olefins can function as active HCP species in zeolites such as the ZSM-5 catalyst with 3-D 10-ring channels and proposed the "dual-cycle" mechanism which greatly enrich the HCP mechanism [30,31].

The carbenium ions are generally known as an important reaction intermediate in the HCP cycle, and the capture and investigation of them also helped a lot in recognition of the MTH reaction. In our laboratory, we directly observed the heptamethylbenzenium cation (heptaMB$^+$) with a newly synthesized SAPO-type DNL-6 molecular sieve with large cavities and the heptaMB$^+$ and pentamethylcyclopentyl cation (pentaMCP$^+$) were also directly observed in CHA-type catalysts during methanol conversion under real working conditions [32,33]. Recently, another group observed several C_5 and C_6-cyclic carbocations and systematically investigated how they participate in the MTH reaction over HZSM-5 catalyst [34,35]. Several three-ring compounds, dienes, polymethylcyclopentenyl and polymethylcyclohexenyl cations were also found and verified as the initial HCP species and the olefin-based catalytic cycle was further proved as the main reaction route during the early stages of the MTO reaction over HSAPO-34 [16].

Despite the great contribution that the HCP mechanism made for understanding of the obvious change of the catalyst activity and the olefin formation mechanism during the MTH process, more research work is still needed for recognition of more detailed reaction behaviour. The MTH reaction is popularly known as an autocatalytic process and the autocatalysis stage can be obviously observed in the induction reaction. However, the induction period is not easily observed under high temperature due to the too rapid reaction rate. We recently found that the induction reaction can be clearly observed and well investigated under low reaction temperature [18,36–38]. Apparently, the autocatalytic methanol conversion during the induction reaction was due to the improvement of catalyst activity on hydrocarbons generation. In detail, factors influencing the catalyst activity are also very complicated, including the reaction temperature, catalyst topologies, contact time, acid properties, etc [36,38–41]. All of these can impose a great impact on the formation of retained species and then the methanol conversion reaction, especially in the MTH induction period.

HZSM-5 and HSAPO-34 are the two most important MTH catalysts and the reaction mechanism in the MTH induction reaction should not be the same due to the different topologies. Considering the importance of the two catalysts for the MTH process, it is very important to carry out a comparative investigation of the MTH induction reaction behaviour over these two catalysts, which is also the main topic of this work. Based on the fixed-bed methanol conversion results and the intelligent gravimetric analyser (IGA) studies, effect of the catalyst topologies on the formation of HCP species and the evolution of the autocatalysis reaction during the MTH induction reaction was systematically investigated.

2. Experimental section

2.1. Preparation of the catalysts

Four HZSM-5 samples (Si/Al = 19, 21, 49 and 99) (the samples were designated as HZ-19, HZ-21, HZ-49 and HZ-99 correspondingly) were obtained from The Catalyst Plant of Nankai University.

HSAPO-34 with two different Si contents were supplied by Group DNL1202 of the Dalian Institute of Chemical Physics, Dalian, China. The two synthesized HSAPO-34 materials with high and low Si contents were named as SA-9 and SA-7.

2.2. Characterization of the catalysts

The powder XRD pattern was recorded on a PANalytical X'Pert PRO X-ray diffractometer with Cu-Kα radiation (λ = 1.54059 Å), operating at 40 kV and 40 mA. The chemical composition of the samples was determined with Philips Magix-601 X-ray fluorescence (XRF) spectrometer. The crystal morphology was observed by field emission scanning electron microscopy (Hitachi, SU8020).

The acid properties were examined by means of the temperature-programmed desorption of ammonia (NH_3-TPD). The experiment was carried out with an Autochem 2920 equipment (Micromeritics). The calcined samples were pretreated at 550 °C for 1 h in He and were then saturated with ammonia at 100 °C for 30 min. After the samples were purged with helium, they were heated at 10 °C min^{-1} from 100 °C to 700 °C.

^{1}H MAS NMR spectroscopy was performed with a Varian Infinity plus-400 spectrometer equipped with a 9.4 T widebore magnet. All the samples were dehydrated at 400 °C and under a pressure

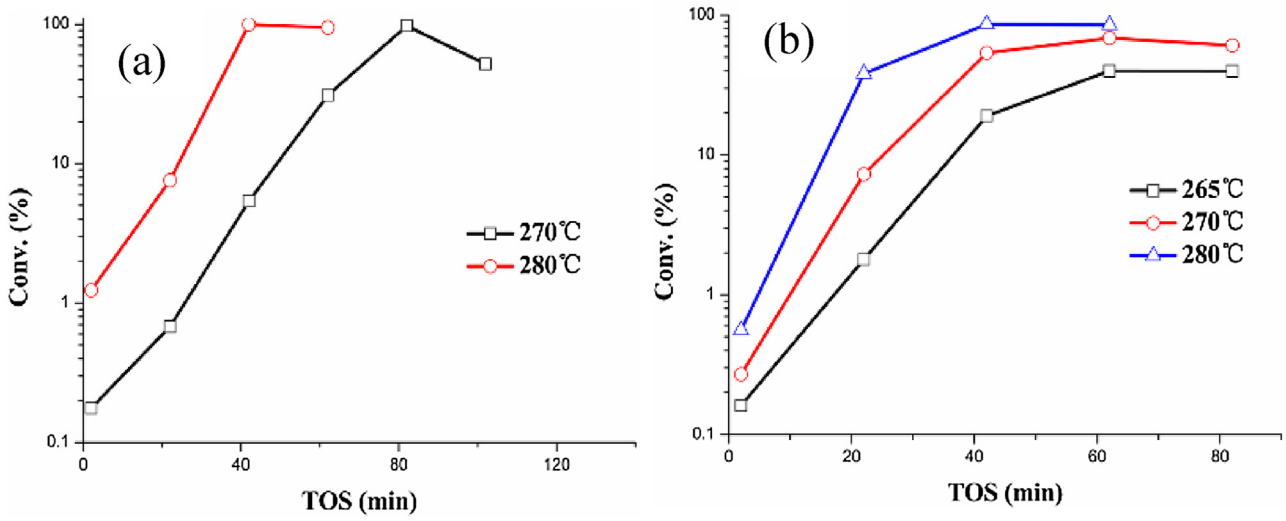

Fig. 2. Conversion of methanol on HZ-19 (a) and SA-9 (b) at different temperature as a function of TOS.

below 10^{-3} Pa for 20 h before the measurements, ^{1}H MAS NMR spectra were recorded through a 4 mm MAS probe and a spin-echo program. The pulse width was 2.2 μs for a π/4 pulse, and 32 scans were accumulated with a 10 s recycle delay.

N_2 adsorption–desorption isotherms were obtained on a Micrometrics ASAP 2020 system at 77 K.

Change of the amount of retained species was in situ monitored by the IGA instrument, model IGA-003, Hiden Analytical Ltd., Warrington, UK. The sensitivity of the balance is 1 μg. Before test, 100 mg of the catalyst materials (40–60 mesh) was placed in the chamber. The samples were pretreated in flowing helium gas until no decrease of catalyst weight was observed and adjusted to the reaction temperature. Then, methanol was fed by passing helium through a saturation evaporator and signals were recorded. The effluent product was analyzed with on-line mass spectra.

2.3. Extraction and GC-MS analysis of the confined organics

Organic compounds trapped in the catalyst was obtained by first dissolving the catalyst (50 mg) in 1.0 mL of 15% HF in a screw-cap Teflon vial and then extracted in 0.5 mL CH_2Cl_2. The organic phase was extracted by CH_2Cl_2, and then analyzed using an Agilent 7890A/5975C GC/MSD.

2.4. Catalytic tests

All samples were pressed into tablets, crushed and sieved into a fraction of 40–60 mesh. The isothermal methanol conversion reactions were performed in a fixed-bed reactor at atmospheric pressure and a catalyst sample of 100 mg was loaded into the reactor. Methanol was fed by passing helium through a saturation evaporator with a WHSV of 2.0 h^{-1}. For the temperature-programmed methanol conversion reaction, a catalyst sample of 1 g was loaded into the reactor. Then quartz sand was added to the upper and lower part of reactor to get a plug flow of the feed. Methanol was pumped into the reactor in a certain and steady velocity (0.085 ml·min^{-1}) to get a space velocity of 4 h^{-1}. For all experiments, catalyst was activated in-situ with an air flow (20 mL min^{-1}) at 550 °C for 1 h before adjusted to predetermined reaction temperature. For the temperature-programmed MTH reaction, the reaction temperature was increased continuously at a heating rate of 0.5 °C min^{-1}.

In order to avoid the product solidification, the outlet line was twined with the heat tape to keep the temperature at 240 °C. The effluent was analyzed by on-line gas chromatography (Angilent GC7890A) equipped with a FID detector and a PoraPLOT Q-HT capillary column. The conversion in this context refers to the percent of methanol converted into hydrocarbons, that is to say, dimethylether is also considered as reactant in the following sections.

3. Results and discussion

3.1. Characterization results of the HZSM-5 and HSAPO-34 catalysts

Powder XRD confirmed that all the HZSM-5 and HSAPO-34 catalysts consisted of a well crystalline MFI and CHA phase correspondingly (Fig. S1). Fig. S2 shows the SEM photos of the HZSM-5 catalysts and the crystallite shapes as well as the crystallite sizes were similar with each other, with average crystallite sizes of 1.0-2.0 um for all samples. For HSAPO-34 catalysts, the crystallite shapes as well as the crystallite sizes were also almost the same, with crystallite sizes of about 10 um for the two samples (Fig. S3).

The chemical composition and the BET results of all HZSM-5 samples were given in Table S1. It can be seen from the BET results that all the four HZSM-5 samples has similar micropore and external surface area, and very similar micropore and mesopore pore volume, demonstrating the identical diffusivity of the four HZSM-5 catalysts. The same characterization results for HSAPO-34 are given in Table S2 and no obvious physical character difference can be observed for the two samples.

NH_3-TPD and ^{1}H MAS NMR experiments were also carried out to characterize the acid property of the HZSM-5 and HSAPO-34 catalysts. The TPD profiles for the HZ-19, −21, −49, −99 catalysts are presented in Fig. S4 (a), two desorption peaks at a low and a high temperature were clearly recognized, corresponding to weak and strong acid sites, respectively. The desorption peak area of the TPD curve decreased with increasing of Si/Al ratio, presenting the decrease of the acid site density. Moreover, it should be noted that both the weak and strong peak centers shifted to lower temperature as the Si/Al ratio increases indicating the decrease of acid strength for these two kinds of acid sites. Distribution of the weak and strong acid sites for HZSM-5 catalysts with different Si/Al ratio can be seen in Table S3. It can be seen that there existed a little difference for the weak and strong acid sites distribution, and the ratio of the weak acid site was relatively higher for HZ-49 and HZ-99 catalysts. The ^{1}H MAS NMR results are presented in Fig. S5. It can

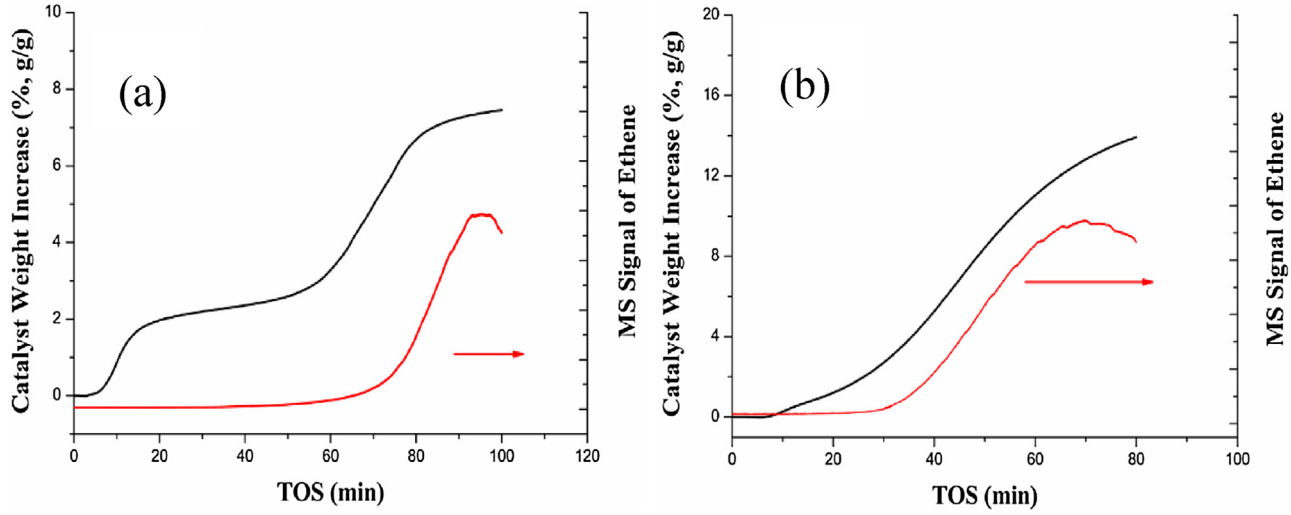

Fig. 3. IGA studies in the MTH reaction at 275 °C over HZ-19 (a) and SA-9 (b) catalysts.

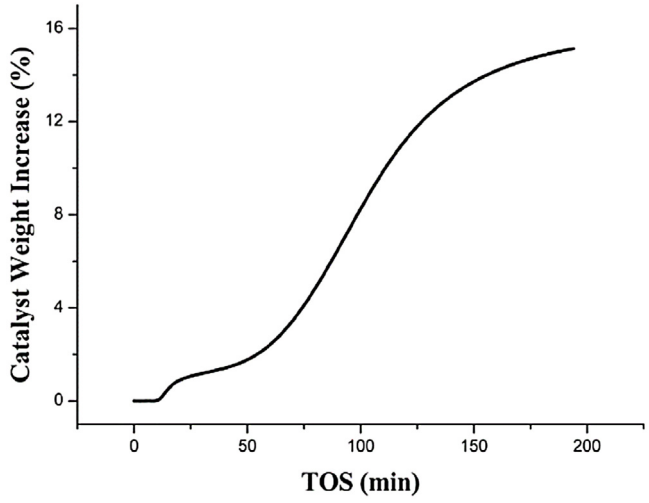

Fig. 4. IGA studies in the MTH reaction at 265 °C for SA-9 catalysts.

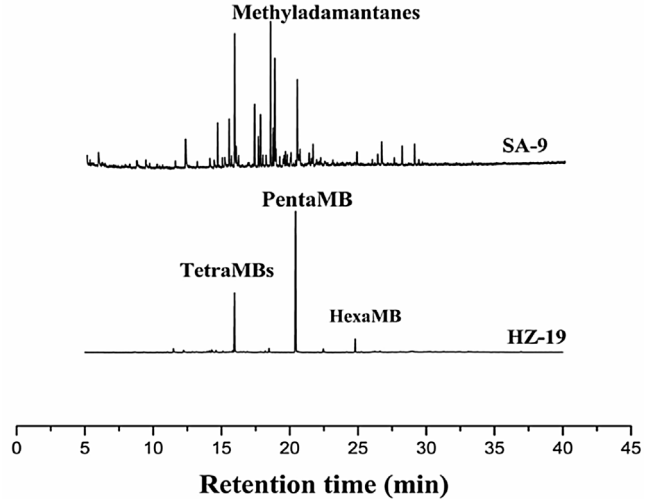

Fig. 5. GC-MS analysis of retained species after methanol conversion at 270 °C for 42 min over HZ-19 and 62 min over SA-9.

be seen that the main difference of HZSM-5 catalysts with different Si/Al ratios was the acid site density and it decreased continuously with the increase of Si/Al ratio (Fig. S4 (a) and Fig. S5 (a), Table S1). For HSAPO-34 catalysts, the acid strength was similar and the acid site density decreased with the decrease of the Si content (Table S2 and Fig. S5 (b)). The acid strength of HZSM-5 was stronger than that of HSAPO-34 catalyst.

3.2. Different induction reaction behaviour over HZSM-5 and HSAPO-34 catalysts under low temperature

3.2.1. Increase of methanol conversion with TOS

The MTH reactions were firstly performed over HZ-19 and SA-9 catalysts at 260 °C. It can be seen from Fig. 1(a) that there exists an obvious induction period for both catalysts. To investigate the MTH induction more clearly, the methanol conversion was also plotted against time on stream (TOS) in a logarithmic scale in Fig. 1(b). For HZ-19 catalyst, the initial two stages were clearly presented, the existence of which has been proved in the previous work [18]. After the very initial stage, the autocatalysis reaction can be observed — a perfect straight line from 22 to 162 min over HZ-19 catalyst. Due to the stronger acid strength of HZ-19, the initial methanol conversion at 2 min was higher than that over SA-9. However, the MTH reaction seemed to be initiated much easier over the HSAPO-34 sample. Because of the higher acid site density over HSAPO-34 catalyst, the initial HCP species can be generated much easier in the HSAPO-34 cages than in the HZSM-5 channel intersections and they may be more actively involved in the catalytic cycle over HSAPO-34 catalyst. Consequently, the initial two stages was too short to be observed over the SA-9 catalyst under current condition and the autocatalysis stage can be observed since the very beginning of the induction reaction. It should be noted that, the increase of the methanol conversion was quite different for the SA-9 catalyst. In Fig. 1(b), it can be seen that the change of methanol conversion with TOS was not always a straight line in the whole induction reaction process. The real autocatalytic reaction can only be observed before 40 min, after which the increasing rate of methanol conversion lowered down gradually.

By increasing the reaction temperature, the initial two stages became too short to be observed for HZ-19 catalyst (Fig. 2(a)). Both the methanol conversion and its increasing rate became higher at higher temperature but the increasing of methanol conversion with TOS was always a straight line before deactivation (Fig. 2(a)). While for HSAPO-34 catalyst, despite the higher increasing rate of methanol conversion at higher temperature, it always slowed down

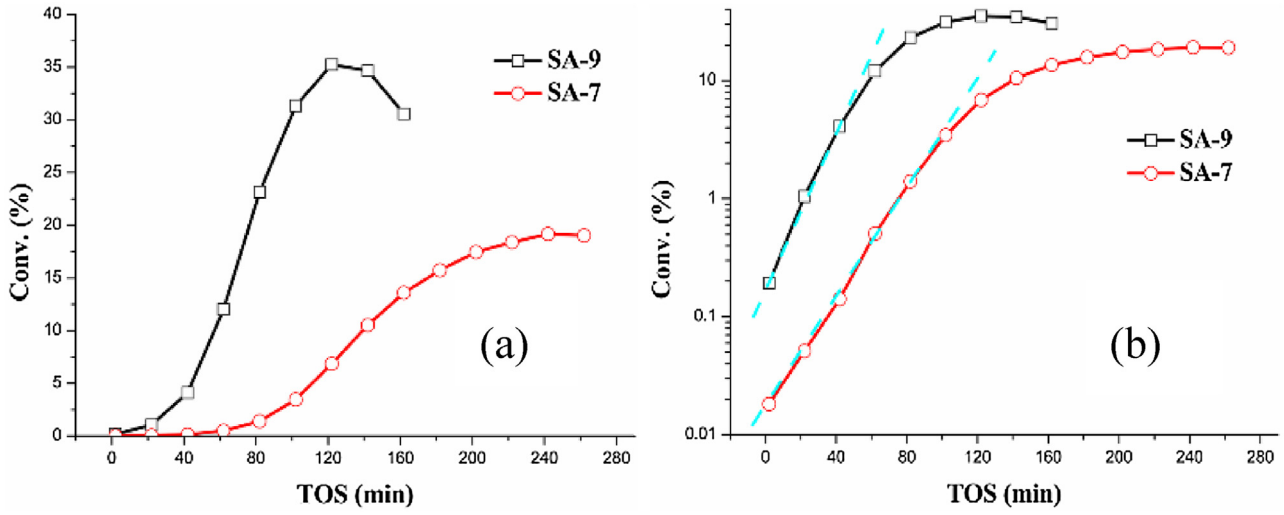

Fig. 6. Conversion of methanol on SA-7 and SA-9 at 260 °C as a function of TOS. The y axis is in a normal linear scale for (a) and a logarithmic scale for (b).

in the latter stage of the induction period and that occurred much earlier at higher temperature.

3.2.2. IGA studies during the induction period

The changing amount of the retained species was continuously monitored with IGA analysis over these two catalysts. The IGA equipment is quite sensitive to the change of catalyst weight (CW) (1 μg). For both catalysts, it can be seen that the CW increased continuously once methanol was fed into the reactor (Fig. 3). It was also clearly seen that the increase of CW with TOS can be clearly divided into three stages for HZSM-5 catalyst. According to our recognition of the MTH reaction, the first stage may be caused by adsorption of methanol and formation of surface methoxy species; the second stage was for the gradual accumulation of the initial HCP species and no obvious ethene signal can be detected in this stage; the third stage was due to the rapid accumulation of retained species, obvious ethene signal was observed and increased rapidly with TOS. The three-staged change of CW with TOS was in well accordance with our previous finding that the change of methanol conversion with TOS can be divided into three stages: the initial reaction stage, the initial HCP species formation stage and the autocatalysis stage [18]. Change of the mass spectra signal of ethene with the CW change can also be obviously observed since the start of the third reaction stage. This further demonstrated that the change of catalyst activity was closely related with the formation of the retained species.

The increase of CW with TOS was quite different for HSAPO-34 catalyst. The initial two stages can not be obviously observed due to the rapid initiation of the autocatalysis reaction. It may be because that the surface methoxy can be quickly involved into the methanol conversion reaction and was easily consumed. Moreover, from the change of mass spectra signal of ethene, it can be seen that the autocatalysis reaction was initiated much earlier and easier for SA-9 catalyst. By lowering down the reaction temperature to 265 °C, the CW increase of SA-9 slowed down, the consumption rate of surface methoxy decreased and the initial two stages could be clearly presented in Fig. 4.

3.2.3. Reasons for the different induction reaction behaviour under isothermal conditions

According to the HCP mechanism, the increase of methanol conversion should be closely related with the formed organic species retained in the catalyst cages or intersections, especially during the induction period. The different induction reaction behaviour over HZSM-5 and HSAPO-34 catalysts presented in Fig. 1 may be caused by the different amount of retained species or their different activity. It can be seen from the IGA results that, the CW value increased faster and was higher for the HSAPO-34 than HZSM-5 catalyst. Generally speaking, during the induction period, faster formation rate of retained species may indicate faster methanol conversion increasing rate. As a result, it can be deduced that the retarded autocatalytic reaction for SA-9 catalyst may be caused by the formation of inactive species.

The retained species generated in the MTH induction reaction was further analysed. The GC-MS analysis (Fig. 5) showed that, the dominated retained species were tetramethylbenzenes (tetraMBs) and pentamethylbenzene (pentaMB) over HZ-19 catalyst, which have been proved to be the major active HCP species [34,35]. However, over SA-9 catalyst, besides a certain amount of pentaMB and hexamethylbenzene (hexaMB), large amount of inactive methyladamantanes were also detected [42].

Thus it can be concluded that the generation of the retained species was much easier over the CHA-type HSAPO-34 catalyst, which brought about the easier initiation of the autocatalysis reaction. However, the composition of the generated retained species was quite different for HZSM-5 and HSAPO-34 catalyst due to their different topologies. For HZSM-5 catalyst, the major retained species were active methylbenzenes which can accelerate the methanol conversion, while for HSAPO-34 catalyst, both the active and inactive species were simultaneously generated during the induction reaction and the inactive species was the major constituent. Too much inactive methyladamantanes retained in the cages of HSAPO-34 would lead to severe diffusion limitations and slow down the methanol conversion rate.

3.3. MTH induction reaction over HZSM-5 catalysts with different Si/Al ratios and HSAPO-34 catalysts with different Si contents

3.3.1. MTH induction reaction over HSAPO-34 catalysts with different Si contents

As an acid-catalyzed reaction, the formation of the retained species should be very sensitive to the acid characters of catalysts and that can be reflected through the MTH induction reaction behaviour. The acid site density of HSAPO-34 material is closely related with the Si content and is higher for catalyst with higher Si content (Fig. S5 (b) and Table S2). For MTH reaction over SA-7 and SA-9 catalysts under the same reaction condition, it was found that the initiation of the autocatalysis reaction was much easier for SA-9 catalyst with higher acid site density (Fig. 6(a)). Moreover, the

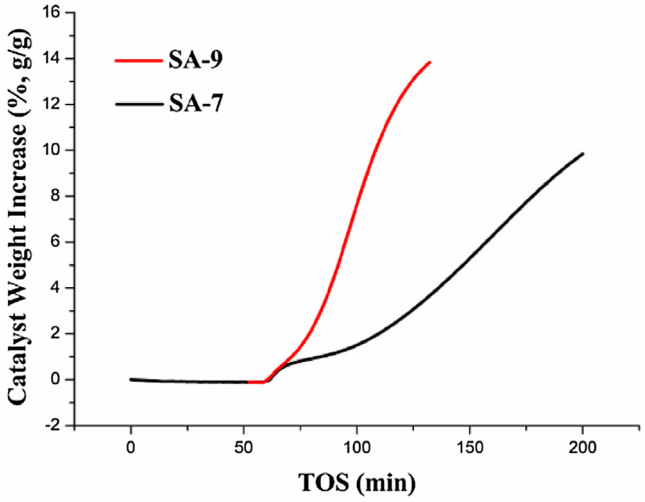

Fig. 7. IGA studies in the MTH reaction at 275 °C over SA-7 and SA-9 catalysts.

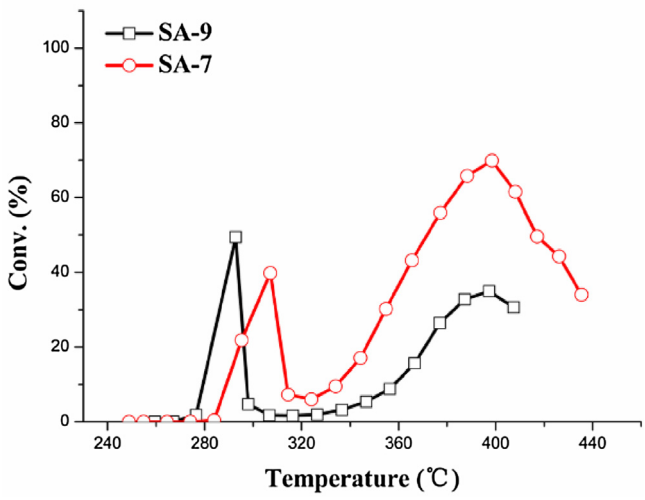

Fig. 8. Methanol conversion as a function of temperature during the TP-MTH reaction over SA-7 and SA-9 catalysts.

increasing rate of methanol conversion was also higher for SA-9 catalyst (Fig. 6(b)). The IGA studies were further performed over SA-7 and SA-9 catalysts for a detailed comparison. The initial two stages can be observed over SA-7 catalyst, indicating that the formation of the initial HCP species became difficult over catalyst with lower acid site density. It can be seen from Fig. 7 that both the amount and the increasing rate of CW was higher for SA-9 catalyst. This corresponded with the result in Fig. 6 very well and further consolidate that the formation of retained species can be promoted by increasing the acid site density.

As we mentioned above, both active and inactive retained species were generated in the induction reaction over HSAPO-34 catalyst and too much accumulation of the inactive methyladamantanes would slow down the increasing rate of methanol conversion and finally brought about the catalyst deactivation. It can be clearly seen that the real autocatalysis reaction (the blue dotted line in Fig. 6(b)) can last longer for SA-7 catalyst (102 min > 42 min). Besides, the decreasing rate also slowed down in the latter stage of the induction period for SA-7 sample. It can be attributed to that, the increase of the acid site density can not only enhance the formation of active HCP species but also promote the generation of inactive species.

The induction reaction during the temperature-programmed methanol conversion (TP-MTH) reaction was further investigated. This is also an important and interesting issue for the MTH industry due to that the low reaction temperature cannot be avoid for starting up operation of an industrial unit. According to the previous research, there existed an obvious deactivation behaviour during the TP-MTH reaction over HSAPO-34 catalyst due to the formation of methyladamantanes [41]. The deactivated catalyst can partly recover its activity with the increase of temperature since the inactive methyladamantanes can be transformed into active methylnaphthalenes at higher temperature.

The TP-MTH reactions were carried out over SA-9 and SA-7 catalysts. It can be seen from Fig. 8 that the initiation of the autocatalysis reaction was much easier for SA-9 catalyst with higher acid site density, which was consistent with the isothermal reaction result. For both catalysts, there existed an obvious deactivation behaviour at around 300 °C due to the accumulation of too much methyladamantanes. After that, the catalyst activity gradually recovered and finally became deactivated again at around 400 °C.

For a better understanding of the TP-MTH process over HSAPO-34 catalysts, the IGA studies were also performed under the temperature-programmed condition. Taking the experiment result in Fig. 8 and 9 and into consideration, it can be understood that the

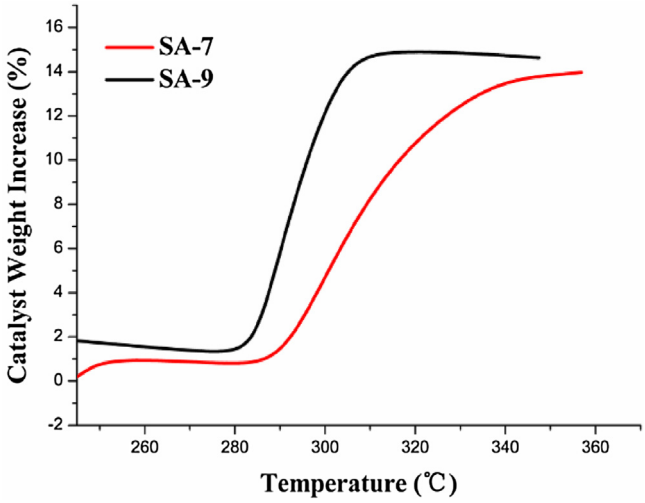

Fig. 9. IGA studies in the TP-MTH reaction over SA-7 and SA-9 catalysts.

easier initiation of the MTH reaction was caused by the easier formation of retained species for SA-9 catalyst. At the same time, large amount of inactive methyladamantanes was inevitably generated, causing serious block of the catalyst cages and leaded to the deactivation. Because of the lower acid site density, the accumulation rate of the retained species lowered down, the deactivation behaviour appeared later and the recovery of the catalyst activity was much easier after the deactivation point for SA-7 catalyst.

3.3.2. MTH induction reaction over HZSM-5 catalysts with different Si/Al ratios

The Si/Al ratio of HZSM-5 samples is closely related with their acid property and the acid site density is higher for that with lower Si/Al ratio (Fig. S5 (a), Table S1). Comparative investigation of the MTH induction reactions has been performed over HZ-19, 49, and 99 catalysts under isothermal reaction conditions. The reaction rate increased continuously with the decrease of Si/Al ratios, indicating that higher acid site density favour the formation of retained species [36]. Moreover, it should be mentioned that the methanol conversion reaction during the induction period under low reaction temperature was a better autocatalysis reaction compared with the HSAPO-34 catalysts.

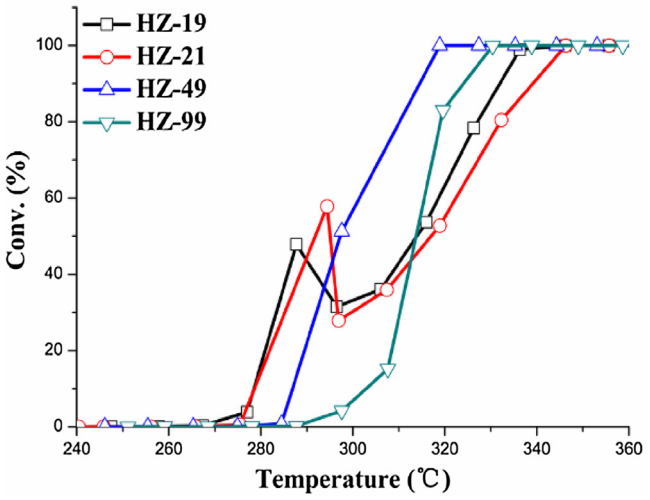

Fig. 10. Methanol conversion as a function of temperature during the TP-MTH reaction over HZ-19, 21, 49 and 99 catalysts.

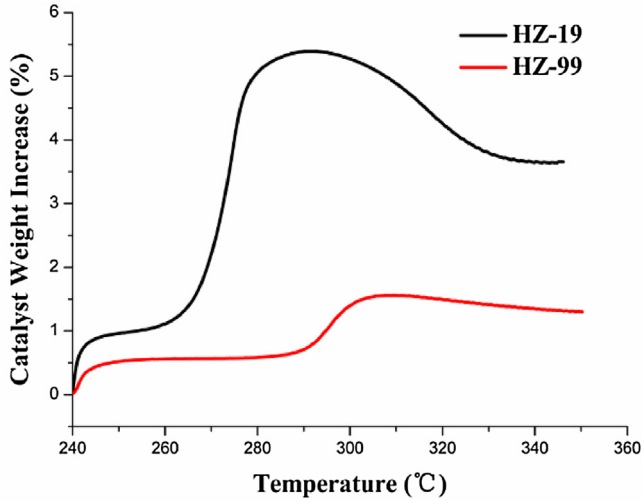

Fig. 11. IGA studies in the TP-MTH reaction over HZ-19 and HZ-99 catalysts.

Influence of Si/Al ratios on the TP-MTH reaction over HZSM-5 catalysts was further investigated and the IGA studies were also performed to monitor the change of the amount of the retained species under the temperature-programmed condition. Change of methanol conversion with TOS is presented in Fig. 10. It can be seen that the initiation of the methanol conversion was relatively easier and thus the autocatalysis reaction could start at lower temperature over catalysts with lower Si/Al ratios. Moreover, a similar deactivation behaviour with that over the HSAPO-34 catalysts can also be observed over HZSM-5 catalysts with lower Si/Al ratios (HZ-19, 21) but disappeared over ones with higher Si/Al ratios (HZ-49, 99). Due to the similar observed reaction behaviour for HZ-19 and HZ-21, HZ-49 and HZ-99. HZ-19 and HZ-99 catalysts were selected for the comparative IGA studies. The changing amount of the retained species during the TP-MTH process is clearly presented in Fig. 11. The CW value was higher for HZ-19 catalyst during the initial two stages due to the more generated surface methoxy species over more acid sites. Besides, the initial two stages was shortened, demonstrating that the formation of the retained species was much easier and quicker over HZ-19 catalyst and that can be accountable for the easier initiation of the autocatalysis reaction. The maximum amount of the retained species for HZ-19 was almost five times of that for HZ-99. Besides, for both samples, the amount of the retained species firstly increased and then decreased at higher temperature. This demonstrated that, higher acid site density can promote the methanol conversion reaction with more rapid generation of the retained species. However, too much accumulated retained species could also lead to the unexpected deactivation for the HZSM-5 catalyst under low temperature.

3.4. Discussion for the MTH induction reaction behaviour over HZSM-5 and HSAPO-34

Taking the above experimental results into consideration, it can be concluded that the MTH induction reaction behaviour is closely related with the formation of the retained species in the catalyst cages or channel intersections. Moreover, the generation of the retained species has an intimate relationship with the catalyst topologies and the acid characters. Combined the fixed-bed reaction results with the IGA results, it can be directly observed that the initiation of the MTH reaction was much easier over HSAPO-34 catalyst which may be caused by the higher acid site density and the spatial confinement effect of the CHA cages. For HSAPO-34 catalyst, both the active methylbenzenes and the inactive methyladamantanes are simultaneously generated during the induction reaction and the accumulation of the latter one will lead to the decrease of the methanol conversion increasing rate.

In the latter stage of the MTH induction reaction. However, for HZSM-5 catalyst, due to the continuous generation of active methylbenzenes and the better diffusion property of the MFI topology (HZSM-5 with the MFI topology is featured with a 3D network consisting of sinusoidal ($5.1 \times 5.5\,Å^2$) and straight ($5.3 \times 5.6\,Å^2$) 10-rings channels, while HSAPO-34 with the CHA topology, is featured with spacious cavities ($10 \times 6.7\,Å^2$) connected by small ($3.8 \times 3.8\,Å^2$) 8-ring windows.), the increase of the methanol conversion with TOS is a well-defined autocatalysis reaction during the whole induction period. Increase of the acid site density can shorten the MTH induction period for both HZSM-5 and HSAPO-34 catalysts. For HSAPO-34 catalyst, the higher acid site density can not only promote the generation of active HCP species but also enhance the inactive species formation which finally leaded to an earlier deactivation.

For HSAPO-34 with different Si contents, the TP-MTH reaction behaviour was almost the same, both are accompanied with an obvious deactivation at around 300 °C. The deactivation behaviour appeared later and the recovery of the catalyst activity after that was easier for the low-silica sample due to the less formed methyladamantanes. For HZSM-5 catalysts, the deactivation behavior can only be observed over samples with low Si/Al ratios under current conditions due to the obviously different formation rate of retained species.

For the IGA studies under TP-MTH reaction, it can be seen that for both HZSM-5 and HSAPO-34, the formation of the retained species was easier for samples with higher acid site density. However, the evolution process of the retained species formation was quite different for HZSM-5 and HSAPO-34 catalysts. The amount of the retained species continuously increased until reached a stable value over HSAPO-34 catalyst. While for HZSM-5, the amount of retained species firstly increased and then decreased to a constant value. It is because that the generated methyladamantanes can not diffuse out of the CHA cages due to its small pore size and can only be transformed into heavier polycyclic species with the increase of temperature. While for HZSM-5 catalyst, due to the larger pore size of the zeolite channels, when the methylbenzenes were cracked with temperature increase, the smaller ones can diffuse out of the channels and the catalyst activity can be easily recovered.

4. Conclusions

The comparative investigation of MTH induction reaction was performed over HZSM-5 and HSAPO-34 catalysts combined with the IGA studies. After initiation of the reaction, the MTH induction reaction over HZSM-5 catalyst was a well-defined autocatalysis reaction. Compared with HZSM-5, the initiation of the MTH reaction was easier over HSAPO-34 catalyst but the increase of methanol conversion was retarded at the latter stage due to the accumulation of methyladamantanes. Increase of the acid site density can promote the formation of retained species for both the HZSM-5 and HSAPO-34 catalysts. There existed an similar deactivation behaviour for both HZSM-5 catalysts with low Si/Al ratios and HSAPO-34 catalysts during the TP-MTH reaction. The difference in TP-methanol conversion study in combination of online TG analysis were closely related with the confined organics formation and transformation. With temperature increase, the confined organics formed at low temperature could be removed from the channel of HZSM-5, but these species retained in the cage of SAPO-34 with 8-ring pore opening, corresponding to the difference of catalyst weight change. All these findings helped reveal the important influence of catalyst topologies on the formation of retained species and then on the catalyst activity during the MTH induction reaction.

Appendix A. Supplementary data

Supplementary data associated with this article can be found, in the online version, at http://dx.doi.org/10.1016/j.mcat.2017.02.018.

References

[1] M. Stocker, Micropor. Mesopor. Mat. 29 (1999) 3–48.
[2] J.F. Haw, W.G. Song, D.M. Marcus, J.B. Nicholas, Accounts Chem. Res. 36 (2003) 317–326.
[3] U. Olsbye, S. Svelle, M. Bjorgen, P. Beato, T.V.W. Janssens, F. Joensen, S. Bordiga, K.P. Lillerud, Angew Chem. Int. Ed. 51 (2012) 5810–5831.
[4] P. Tian, Y.X. Wei, M. Ye, Z.M. Liu, ACS Catal. 5 (2015) 1922–1938.
[5] P. Salvador, J.J. Fripiat, J. Phys. Chem.-Us 79 (1975) 1842–1849.
[6] P. Salvador, W. Kladnig, J. Chem. Soc. Farad. T. 1 (73) (1977) 1153–1168.
[7] E.G. Derouane, P. Dejaifve, J.B. Nagy, J. Mol. Catal. 3 (1978) 453–457.
[8] J. Novakova, L. Kubelkova, K. Habersberger, Z. Dolejsek, J. Chem, Soc. Farad. T. 1 (80) (1984) 1457–1465.
[9] J. Novakova, L. Kubelkova, Z. Dolejsek, J. Catal. 108 (1987) 208–213.
[10] S.R. Blaszkowski, R.A. vanSanten, J. Am. Chem. Soc. 119 (1997) 5020–5027.
[11] N. Tajima, T. Tsuneda, F. Toyama, K. Hirao, J. Am. Chem. Soc. 120 (1998) 8222–8229.
[12] D. Lesthaeghe, V. Van Speybroeck, G.B. Marin, M. Waroquier, Chem. Phys. Lett. 417 (2006) 309–315.
[13] D. Lesthaeghe, V. Van Speybroeck, G.B. Marin, M. Waroquier, Angew. Chem. Int. Ed. 45 (2006) 1714–1719.
[14] H. Yamazaki, H. Shima, H. Imai, T. Yokoi, T. Tatsumi, J.N. Kondo, J. Phys. Chem. C 116 (2012) 24091–24097.
[15] J.F. Li, Z.H. Wei, Y.Y. Chen, B.Q. Jing, Y. He, M. Dong, H.J. Jiao, X.K. Li, Z.F. Qin, J.G. Wang, W.B. Fan, J. Catal. 317 (2014) 277–283.
[16] W.L. Dai, C.M. Wang, M. Dyballa, G.J. Wu, N.J. Guan, L.D. Li, Z.K. Xie, M. Hunger, ACS Catal. 5 (2015) 317–326.
[17] Y. Liu, S. Muller, D. Berger, J. Jelic, K. Reuter, M. Tonigold, M. Sanchez-Sanchez, J.A. Lercher, Angew. Chem. Int. Ed. 55 (2016) 5723–5726.
[18] L. Qi, Y.X. Wei, L. Xu, Z.M. Liu, ACS Catal. 5 (2015) 3973–3982.
[19] T. Mole, J. Catal. 84 (1983) 423–434.
[20] T. Mole, G. Bett, D. Seddon, J. Catal. 84 (1983) 435–445.
[21] T. Mole, J.A. Whiteside, D. Seddon, J. Catal. 82 (1983) 261–266.
[22] I.M. Dahl, S. Kolboe, J. Catal. 149 (1994) 458–464.
[23] S.R. Blaszkowski, R.A. Vansanten, J. Phys. Chem.-Us. 99 (1995) 11728–11738.
[24] J.F. Haw, J.B. Nicholas, W.G. Song, F. Deng, Z.K. Wang, T. Xu, C.S. Heneghan, J. Am. Chem. Soc. 122 (2000) 4763–4775.
[25] W.G. Song, J.F. Haw, J.B. Nicholas, C.S. Heneghan, J. Am. Chem. Soc. 122 (2000) 10726–10727.
[26] S. Teketel, U. Olsbye, K.P. Lillerud, P. Beato, S. Svelle, Micropor. Mesopor. Mat. 136 (2010) 33–41.
[27] I.M. Dahl, S. Kolboe, Catal. Lett. 20 (1993) 329–336.
[28] I.M. Dahl, S. Kolboe, J. Catal. 161 (1996) 304–309.
[29] R.F. Sullivan, R.P. Sieg, G.E. Langlois, C.J. Egan, J. Am. Chem. Soc. 83 (1961) 1156.
[30] S. Svelle, F. Joensen, J. Nerlov, U. Olsbye, K.P. Lillerud, S. Kolboe, M. Bjorgen, J. Am. Chem. Soc. 128 (2006) 14770–14771.
[31] M. Bjorgen, S. Svelle, F. Joensen, J. Nerlov, S. Kolboe, F. Bonino, L. Palumbo, S. Bordiga, U. Olsbye, J. Catal. 249 (2007) 195–207.
[32] J.Z. Li, Y.X. Wei, J.R. Chen, P. Tian, X. Su, S.T. Xu, Y. Qi, Q.Y. Wang, Y. Zhou, Y.L. He, Z.M. Liu, J. Am. Chem. Soc. 134 (2012) 836–839.
[33] S.T. Xu, A.M. Zheng, Y.X. Wei, J.R. Chen, J.Z. Li, Y.Y. Chu, M.Z. Zhang, Q.Y. Wang, Y. Zhou, J.B. Wang, F. Deng, Z.M. Liu, Angew. Chem. Int. Ed. 52 (2013) 11564–11568.
[34] C. Wang, Y.Y. Chu, A.M. Zheng, J. Xu, Q. Wang, P. Gao, G.D. Qi, Y.J. Gong, F. Deng, Chem.-Eur. J. 20 (2014) 12432–12443.
[35] C. Wang, J. Xu, G.D. Qi, Y.J. Gong, W.Y. Wang, P. Gao, Q. Wang, N.D. Feng, X.L. Liu, F. Deng, J. Catal. 332 (2015) 127–137.
[36] L. Qi, J.Z. Li, Y.X. Wei, Y.L. He, L. Xu, Z. Liu, Rsc Adv. 6 (2016) 52284–52291.
[37] L. Qi, J.Z. Li, Y.X. Wei, L. Xu, Z.M. Liu, Catal. Sci. Technol. 6 (2016) 3737–3744.
[38] L. Qi, J.Z. Li, L. Xu, Z.M. Liu, Rsc Adv. 6 (2016) 56698–56704.
[39] Y.X. Wei, D.Z. Zhang, F.X. Chang, Z.M. Liu, Catal. Commun. 8 (2007) 2248–2252.
[40] E. Borodina, F. Meirer, I. Lezcano-Gonzalez, M. Mokhtar, A.M. Asiri, S.A. Al-Thabaiti, S.N. Basahel, J. Ruiz-Martinez, B.M. Weckhuysen, ACS Catal. 5 (2015) 992–1003.
[41] C.Y. Yuan, Y.X. Wei, J.Z. Li, S.T. Xu, J.R. Chen, Y. Zhou, Q.T. Wang, L. Xu, Z.M. Liu, Chin. J. Catal. 33 (2012) 367–374.
[42] Y.X. Wei, J.Z. Li, C.Y. Yuan, S.T. Xu, Y. Zhou, J.R. Chen, Q.Y. Wang, Q. Zhang, Z.M. Liu, Chem. Commun. 48 (2012) 3082–3084.